Eur. Phys. J. B **53**, 307–313 (2006)
DOI: 10.1140/epjb/e2006-00393-4

THE EUROPEAN PHYSICAL JOURNAL B

Magnetization scaling in the ruthenate-cuprate $RuSr_2Eu_{1.4}Ce_{0.6}Cu_2O_{10-\delta}$ (Ru-1222)

S. Garcia[1,2,a], L. Ghivelder[1], S. Soriano[1], and I. Felner[3]

[1] Instituto de Física, Universidade Federal do Rio de Janeiro, C.P. 68528, Rio de Janeiro, RJ 21941-972, Brazil
[2] Laboratorio de Superconductividad, Facultad de Física-IMRE, Universidad de La Habana, San Lázaro y L, Ciudad de La Habana 10400, Cuba
[3] Racah Institute of Physics, The Hebrew University, Jerusalem, 91904, Israel

Received 30 May 2006 / Received in final form 6 September 2006
Published online 27 October 2006 –

Abstract. The magnetic properties of the superconducting ruthenate-cuprate $RuSr_2Eu_{1.4}Ce_{0.6}Cu_2O_{10-\delta}$ (Ru-1222) have been studied by a scaling analysis of the dc magnetization and ac susceptibility measurements. Non-linear $M(H)$ curves reveal the presence of nano-size clusters with a net magnetic moment of $\sim 10^2$ μ_B at 180 K, near the deviation from a Curie-Weiss behavior. On cooling, no scaling was observed down to 90 K, discarding the possibility of magnetic phase separation of collinear ferromagnetic particles. We explain this result in terms of a variable number of contributing particles, with a temperature dependent net magnetic moment. For 70 K $\leq T \leq$ 90 K the scaling plots evidence the emergence of a system of non-interacting particles, which couple on further cooling. The observed cluster-glass features are preserved down to the lowest measured temperature (10 K); no signature of long-range order was detected. The frequency shift of the peak in the real part of the ac susceptibility does not follow the Vogel-Fulcher type dependence, as previously reported. The puzzling temperature dependence of the coercive field, $H_C(T)$, is correlated with the changes in the scaling factors.

PACS. 74.25.Ha Magnetic properties – 74.70.Pq Ruthenates

1 Introduction

The magnetic structure of the ruthenate-cuprates $RuSr_2RCu_2O_8$ (Ru-1212) $RuSr_2(R,Ce)_2Cu_2O_{10-\delta}$ (Ru-1222), where R = Gd or Eu, remains a topic of interest and controversy. The details of the magnetic order are relevant for the onset of the superconducting (SC) state and to understand how these two cooperative phenomena accommodate their respective order parameters in the cell volume. Even in the relatively simpler case of Ru-1212, a large discrepancy between different studies is found. Neutron powder diffraction (NPD) measurements reveal an antiferromagnetic (AFM)-like order with a negligible ferromagnetic (FM) moment [1], while magnetization curves, $M(H)$, and nuclear magnetic resonance (NMR) measurements signal a large FM component [2].

The magnetic behavior of Ru-1222 is considerably more complex. NPD studies have not yet provided a definitive answer about the exact magnetic ordering of the Ru moments. Although there is clear evidence of the relevant role played by the crystalline structure in the magnetic response [3], a full understanding of the interplay between the structural features and magnetic order is far from being achieved. Anomalous lattice expansion results [4] and its subsequent retraction [5] added more confusion to this field. Yet another puzzling result is the presence of two magnetic transitions in the temperature dependence of the magnetization, measured with low magnetic fields [6]. The transition at a higher temperature, T_{M1}, is much less intense than that at $T_{M2} < T_{M1}$. Different scenarios have been proposed to interpret these transitions, each consistent with its own experimental data, but a comprehensive understanding requires a careful comparison of studies made by different groups. In the early works [7], it was proposed that *all* Ru moments order antiferromagnetically at T_{M1}, while homogeneous weak-ferromagnetism sets in at T_{M2}, originating from canting of the Ru moments. This canting is a result of the tilting of the RuO_6 octahedra away from the crystallographic c axis, inducing an anti-symmetric exchange coupling of the Dzyaloshisnky-Moriya type [8]. This interpretation is difficult to reconcile with recent ^{57}Fe- and ^{119}Sn-Mössbauer spectroscopy measurements, which show the presence of two distinct magnetic phases [9], as additionally supported by muon spin rotation (μSR) studies [10]. On the other hand, nonlinear $M(H)$ curves at temperatures well above T_{M2} have been reported [11], and ascribed to magnetic phase

[a] e-mail: sgargar2000@yahoo.com.br

separation of FM nanoclusters in an AFM matrix. Under this approach, the emergence of these clusters is a consequence of the competition between FM and AFM interactions, providing a natural scenario for the coexistence of superconductivity and ferromagnetism as spatially separated phenomena. However, this gives no explanation for i) the existence of a peak in the coercive field H_C at $T_{M2} < T < T_{M1}$ [9]; ii) the exact nature of the magnetic transition at T_{M2}, and iii) the shift in temperature of the ac susceptibility peaks as the frequency of the driving field is varied, a signature typical of a spin-glass (SG) [12]. It has been proposed that in Ru-1222 at sufficiently low temperatures, below T_{M2}, the SG phase evolves in to an ordered weak ferromagnetic (WFM) state [12]. The "fortuitous" reduction to zero of H_C in the vicinity of T_{M2} [9], which is a relevant feature linking the magnetic response above and below this temperature, has not yet been understood. The overall results and interpretations signal that the interplay between magnetic frustration, clustering, and long-range canted order are still open issues in Ru-1222.

In this paper we present a detailed investigation of the magnetic response of $RuSr_2Eu_{1.4}Ce_{0.6}Cu_2O_{10-\delta}$, which corresponds to the optimum Ce concentration for the emergence of the SC state [7]. Our aim is focused on understanding some contradictory results previously reported, and explain the puzzling temperature dependence of the coercive field, $H_C(T)$. A careful scaling analysis of the magnetization curves $M(H)$ in a wide temperature interval is conducted. We show that neither magnetic phase separation nor long-range magnetic order are established, and that a cluster-glass state is preserved from T_{M2} down to the lowest temperatures for the majority fraction of the Ru moments (∼90%). At variance with previous reports [14], we found that the proposed Vogel-Fulcher type behavior for the frequency shift in the ac susceptibility χ'-peak, is not actually accomplished. On the contrary, our scaling plots evidence the non-interacting nature (without hysteresis) of the cluster-glass state at T_{M2}. The onset of inter-cluster coupling, revealed by the change in a scaling factor, only occurs about 30 K below T_{M2}, in agreement with the re-opening of the hysteresis in the $M(H)$ curves. In addition, new features were observed in the $M(H)$ curves above T_{M2}: the lack of scaling, an increasing number of contributing nano-size particles on cooling, and a narrow cluster size distribution. These results are ascribed to a minority fraction of Ru moments in the neighborhood of oxygen vacancies.

2 Experimental

The $RuSr_2Eu_{1.4}Ce_{0.6}Cu_2O_{10-\delta}$ sample was prepared following the standard solid-state reaction technique. Stoichiometric amounts of Eu_2O_3, CeO_2, $SrCO_3$, RuO_2, and CuO were mixed, pressed into pellets, and preheated at 1000 °C for 24 hours at atmospheric pressure. The products were cooled, reground and sintered at 1050 °C for 50 hours in a slightly pressurized oxygen atmosphere (∼1.1 atm), and then furnace cooled to room temperature. The X-ray diffraction pattern corresponds to Ru-1222, with no spurious lines observed. The calculated lattice parameters of the tetragonal structure, $a = 3.847(1)$ Å and $c = 28.53(1)$ Å, are in excellent agreement with previously published data [6]. The dc magnetization and ac susceptibility measurements were performed in a Quantum Design PPMS system. Low frequency ac susceptibility, down to 0.01 Hz, was measured with a Cryogenic SQUID magnetometer.

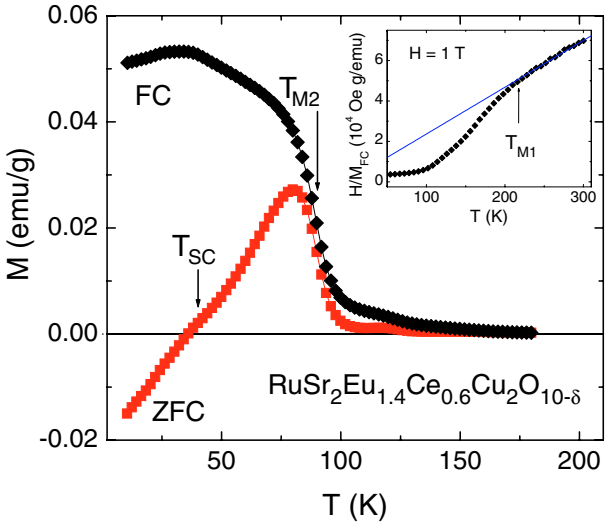

Fig. 1. (Color online) Zero-field-cooled (ZFC) and field cooled (FC) magnetization curves of $RuSr_2Eu_{1.4}Ce_{0.6}Cu_2O_{10-\delta}$, measured with $H = 5$ Oe. The arrows indicate the magnetic transition at $T_{M2} = 90$ K, defined at the inflection point of the FC curve, and the onset of the superconducting state at $T_{SC} \simeq 40$ K. The inset shows the temperature dependence of H/M_{FC}, measured with $H = 1$ T. The temperature T_{M1} marks the onset of the deviation from a Curie-Weiss behavior.

3 Results

The zero-field-cooled and field-cooled-magnetization, M_{ZFC} and M_{FC}, of the Ru-1222 sample is plotted in Figure 1. A small peak is observed around 120 K, while a much stronger rise in the curves appears at 90 K. A signature of the SC transition is the change in slope at $T_{SC} = 40$ K. This is within the upper limit of the transition temperatures reported for Ru-1222, $T_{SC} \simeq 32$–45 K [11,12,9], an indication of the good quality of our sample. The inflection point of the M_{FC} curve is taken as the main magnetic transition, at $T_{M2} = 90$ K, also within the reported range [6,7,9]. A plot of H/M_{FC} vs. T, shown in the inset of Figure 1, reveals a Curie-Weiss behavior down to $T_{M1} \sim 230$ K, followed by a downward deviation on further cooling. No spurious contributions were observed in comparison with previously reported data.

In Figure 2 it is readily observed that all $M(H)$ curves deviate from a linear behavior at temperatures well above T_{M2}, and remain unsaturated even for the highest field

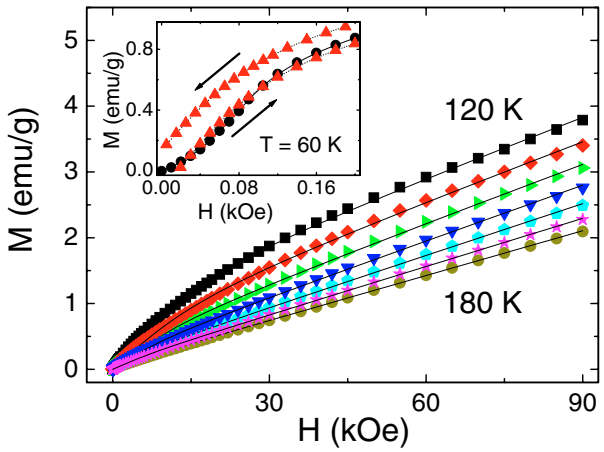

Fig. 2. (Color online) Magnetization vs. applied magnetic field of $RuSr_2Eu_{1.4}Ce_{0.6}Cu_2O_{10-\delta}$, measured, from top to bottom, at T = 120, 130, 140, 150, 160, 170, and 180 K. The solid lines are a fit with a Langevin function plus a linear term [see Eq. (1)]. The inset shows the low-field region of the virgin $M(H)$ curve (closed circles and continuous line) and the hysteresis loop (closed triangle and dotted line), measured at $T = 60$ K.

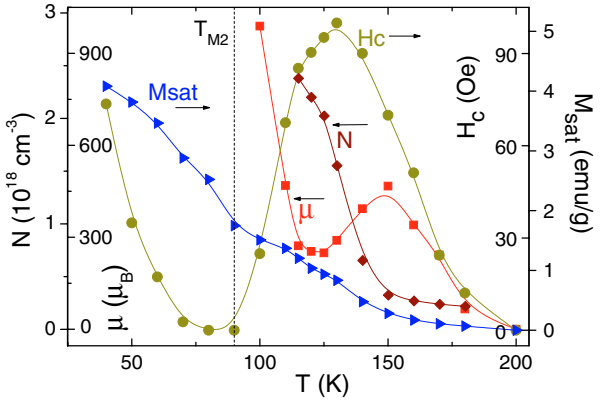

Fig. 3. (Color online) Temperature dependence of the moment of the magnetic clusters μ, saturation magnetization M_{sat}, and density of magnetic clusters per unit volume N, all deduced from the fit of the virgin $M(H)$ curves, and coercive field $H_C(T)$. The lines are a guide to the eyes.

and lowest temperature measured, H = 9 T and T = 10 K. At $T < T_{M2}$, the virgin branches stay outside the hysteresis loop and exhibit an S-type dependence at low fields (Fig. 2, inset); these features disappear above T_{M2}. For $T > T_{M2}$, the virgin branches may be fitted as

$$\chi_0 H + M_{sat}\left[\coth\left(\frac{\mu H}{k_B T}\right) - \frac{k_B T}{\mu H}\right], \qquad (1)$$

which corresponds to a linear term plus a Langevin function, where μ is the magnetic moment of the assumed magnetic clusters, and M_{sat} is the saturation magnetization of this species. A Langevin function has been routinely used when analyzing particle size distribution in granular magnets [15,16] and in manganites [17]. with results which agree well with small-angle neutron scattering [18]. The fitting of the magnetization data with equation (1) is very good over a wide temperature interval above T_{M2}, as shown in Figure 2 for selected temperatures. The deduced parameters of the Langevin-type contribution show a very interesting behavior, and are presented in Figure 3 along with the $H_C(T)$ dependence. The values extracted for μ are of the order of several hundreds μ_B, even at temperatures as high as 180 K, much above T_{M2}. When cooling below T_{M1}, μ rises up to ∼450 μ_B at T = 150 K, diminishes to about 250 μ_B at T = 125 K, remains around this value down to 115 K, and then rapidly increases as T_{M2} is approached. The M_{sat} values exhibit a monotonic increase as the temperature decreases. Taking $\mu(Ru^{5+}) \cong 3\ \mu_B$ [11], M_{sat} at T = 10 K is only of the order of 10% of the total magnetization expected for a collinear FM alignment. Although no jumps were observed in M_{sat} at T_{M2}, its temperature dependence rate increases by a factor of two below this temperature. From the deduced values of M_{sat} and μ, the density of magnetic clusters per unit volume, N, was determined, and also plotted in Figure 3; a monotic increase on cooling is observed The coercive field H_C shows a maximum at 125–130 K, vanishes at T_{M2}, and remains zero down to ∼70 K. On further cooling, a reopening of the hysteresis loops occurs. The fitting of the virgin $M(H)$ branches with a single Langevin function can not be made below T_{M2}. However, M_{sat} can still be determined by fitting a straight line to the high field section of the $M(H)$ curves and subtracting it from the experimental curves. Using this procedure, the deduced M_{sat} values for $T > T_{M2}$ agree within 3–5% with those obtained through the fitting of the Langevin function. The evaluation of M_{sat} for $T < T_{M2}$ is necessary to determine whether the magnetic response in that temperature range follows the scaling laws predicted for granular magnets. The linear term χ_0 reproduces previous reports [6,13], showing a magnitude about a factor of two larger ($\sim 2 \times 10^{-4}$ emu/cm^3) than the contributions coming from the Van Vleck susceptibility of Eu^{3+} ions and the T independent component of the CuO_2 layers ($\sim 8 \times 10^{-5}$ emu/cm^3, Ref. [8]), even at T = 10 K, well below T_{M2}.

Nano-size particles with a net magnetic moment are expected to show a scaling behavior of the reduced magnetization, M/M_{sat}, with $(M_{sat}H)/T$ for non-interacting particles, or with H/M_{sat} for interacting and/or blocked superparamagnetic clusters [15]. However, the M/M_{sat} curves do not scale with neither of the two mentioned factors at $T > T_{M2}$. An excellent scaling with $(M_{sat}H)/T$ was obtained for T = 70, 80, and 90 K, as shown in Figure 4a, where the curves for T = 40 and 60 K are also presented to evidence the continuous departure from this scaling behavior on cooling. We recall that this is just the temperature interval for which H_C becomes zero. Interestingly, as the temperature is decreased further, the M/M_{sat} curves begin to scale with the H/M_{sat} factor, with an excellent agreement for temperatures below 70 K down to 10 K, as shown in Figure 4b; the curves for T = 90 and 100 K are included to illustrate the gradual approach to this scaling law.

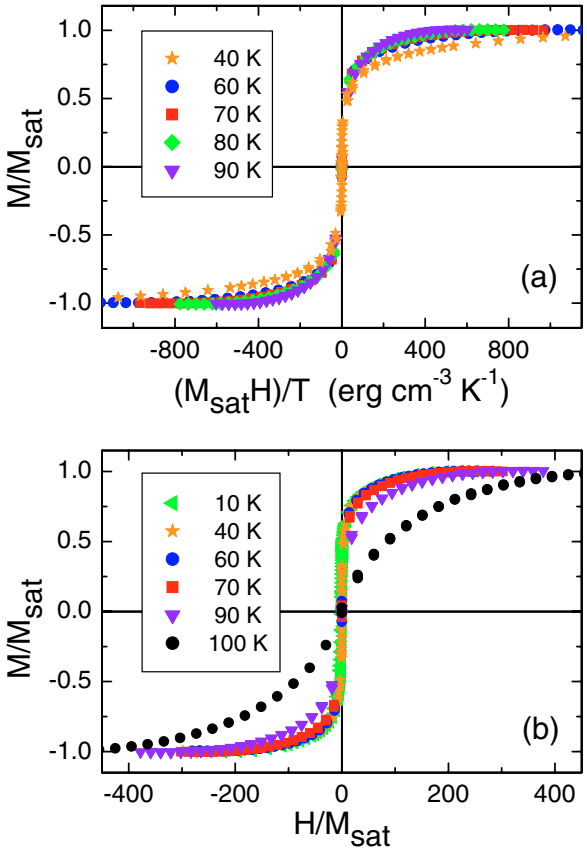

Fig. 4. (Color online) Reduced magnetization of $RuSr_2Eu_{1.4}Ce_{0.6}Cu_2O_{10-\delta}$ at different temperatures ($T <$ 100 K), plotted as a function of $(M_{sat}H)/T$ in (a), and H/M_{sat} in (b).

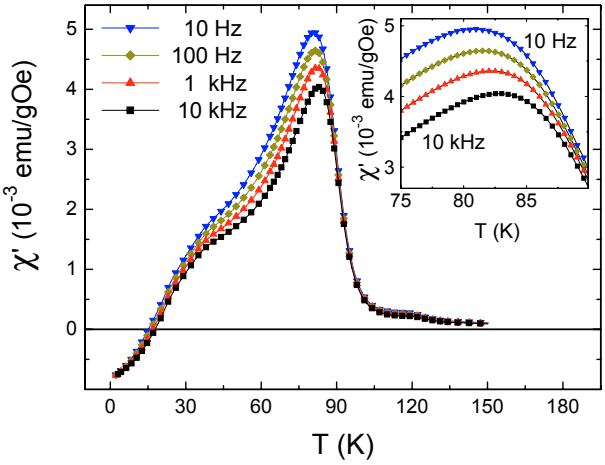

Fig. 5. (Color online) Temperature dependence of the real part of the ac susceptibility, χ', measured at various frequencies with a driving field $h_{ac} = 10$ Oe. The inset shows an enlarged region of the same data.

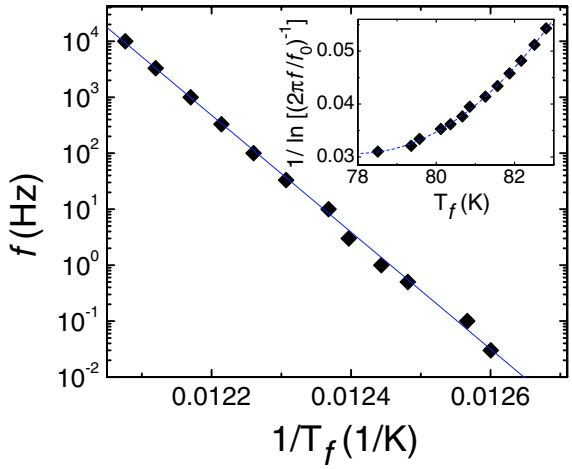

Fig. 6. (Color online) Logarithmic plot of the driving field frequency f vs. the reciprocal of the χ' peak temperature T_f. The solid straight line is an Arrhenius-type fit. The inset shows the variation of $1/\ln[(2\pi f/f_0)]^{-1}$ with the freezing temperature T_f, using $f_0 = 10^{12}$ Hz. The dashed line is a guide to the eyes.

Figure 5 presents the temperature dependence of the real part of the ac susceptibility χ' measured with different frequencies f of the driving field. As in the dc data, a small and smooth peak around 120 K is observed, which does not shift with frequency. The stronger peak, with a maximum at T_f , corresponds to the magnetic transition at T_{M2} (inflection point at 91.5 K). This peak shifts to higher temperatures with decreasing intensity as the frequency is increased (see inset of Fig. 5). This frequency response, the S-type behavior observed in the virgin $M(H)$ branches, and the lack of saturation, are clear signatures of the emergence of a SG state, in agreement with previous results [12,14]. In Figure 6 we show a logarithmic plot of f vs. $1/T_f$. The data clearly follow a linear dependence, which corresponds to an Arrhenius-type expression $f = f_0 \exp(-E_a/k_BT)$, where E_a is the activation energy and f_0 is the characteristic frequency. However, the physically unrealistic values obtained from the linear fitting, $f_0 = 10^{130}$ Hz and $E_a/k_B = 2.4 \times 10^4$ K, indicate that this result needs further consideration. For spin glasses, and also for some paramagnetic systems, deviations from physically acceptable Arrhenius parameters due to coupling between the particles has been treated with a Vogel-Fulcher law [19], expressed by

$$f = f_0 \exp - \left[\frac{E_a}{k_B\,(T - T_0)}\right] \qquad (2)$$

where T_0 is a phenomenological parameter which describes the inter-particle interactions. Equation (2) implies a linear dependence of $1/\ln[(2\pi f/f_0)]^{-1}$ with the freezing temperature T_f. Looking for a better understanding of the frequency response of the ac susceptibility, the $1/\ln[(2\pi f/f_0)]^{-1}$ vs. T_f data were plotted keeping $f_0 = 10^{12}$ Hz as a constant value, which is inside the commonly accepted 10^{11}–10^{13} Hz interval. As shown in the inset of Figure 6, a clear deviation from linearity was obtained. Similar results were obtained with $f_0 = 10^{11}$ and 10^{13} Hz.

4 Discussion

Let us first consider the magnetization measurements above T_{M2}. The large value of μ and its slow decrease with T far above T_{M2} is very different from the $\mu(T)$ behavior for critical fluctuations [20]. Such large μ could be understood on the basis of cluster formation or a strong short-range spin-spin correlation within a coherence volume, as for a cluster-glass state. Nevertheless, the absence of characteristic features of a SG-state for $T > T_{M2}$ excludes this possibility. The small and T dependent M_{sat} values suggest either a homogeneous canted AFM ground state or phase separation, which implies that only a fraction of Ru spins are gradually ferromagnetically aligned. However, a large canting angle is required in the former case ($\approx 20°$) to account for the measured magnetization. Such value is rather unusual in canted AFM structures and agrees with calculations for Ru-1212 [13]. Therefore, the simplest acceptable scenario is the formation of magnetic clusters. Under this assumption, it is expected that the M/M_{sat} curves must scale with the appropriate factors [15]. From the deduced values of N, the volume fraction, $V_F = NV_C$, was determined, where V_C is the average volume of the clusters, assumed spherical. For instance, at $T = 120$ K, $N = 2.2 \times 10^{18}$ cm^{-3}, and $R_C = 24$ Å, where R_C is the average radio of the clusters calculated from the μ values. These results yield a volume fraction V_F of only $\sim$12%, indicating a dilute system of magnetic particles. However, M/M_{sat} does not show the expected scaling with $(M_{sat}H)/T$ above T_{M2}, as expected for non-interacting FM nano-particles. This result is not due to an intercluster coupling, as revealed by the lack of scaling with H/M_{sat}. Since the change from one type of scaling to another is not a sharp transition in granular magnets [15], in principle an intermediary situation is possible. However, the evolution of the scaling features with the decrease in temperature down to 10 K, and the correlation observed between H_C and μ on cooling (as discussed below), clearly evidence that the lack of any scaling behavior for M/M_{sat} above T_{M2} is not due to a weak interaction between collinear FM clusters, but related to a more complex nature of the cluster system. We note that the calculated volume fraction of $\sim$12% at $T = 120$ K is in excellent agreement with the minority magnetic fraction determined through ^{57}Fe- and ^{119}Sn-Mössbauer spectroscopy measurements ($\sim$10%) at this temperature [9] and by muon spin rotation signals [10]. The latter shows that $\sim$15(5)% of the sample volume orders magnetically at $T_{M2} < T < T_{M1}$.

It has been suggested that the presence of clusters above T_{M2} is a consequence of local deviations of oxygen stoichiometry in single-phase Ru-1222, even in well oxygenated samples [21]. They propose the reduction of a fraction of Ru^{5+} ions to Ru^{4+} close to the oxygen vacancies and a stronger Ru^{4+}- Ru^{4+} super-exchange interaction in comparison to Ru^{5+}- Ru^{5+}. We shall re-examine these ideas based on the new results obtained from the $M(H)$ curves above T_{M2}: the lack of scaling behavior, and the fact that the number of contributing particles rises on cooling. In addition, the good fits obtained using a single Langevin function must be explained. The lack of scaling above T_{M2} can be understood as a consequence of the competition between FM and AFM interactions, confined to the Ru^{4+}-rich nano-islands surrounding the oxygen vacancies. This yields a local non-collinear arrangement of the magnetic moments, with a temperature dependent canting angle. When cooling from room temperature, the net magnetic moment increases, reaching $\mu \sim 450\ \mu_B$ at 150 K, and a FM-like hysteresis loop appears due to a spin-flop realignment of the Ru moments as the magnetic field is increased (see Fig. 3). On further cooling, the increase of H_C and the decrease of μ indicate that the AFM interaction between the spins gradually strengthens, until their respective maximum and minimum are reached about 125 K. Once the intracluster canted AFM order is well established, in the vicinity of 125 K, there is no further reduction in μ associated to a progressive anti-parallel alignment. The magnetic moment of the clusters remains almost constant, $\mu \sim 250\ \mu_B$, in a narrow temperature range down to 115 K. At $T = 100$–110 K an increase in μ is observed, suggesting the growth of the clusters. The simultaneous decrease of H_C seems to confirm this idea, if the clusters are now so large that they are no longer single-domain particles. However, even with an increase in μ up to $\sim$1000 μ_B at 100 K the size of the clusters remain at a nanometric scale ($R_C \sim 40$ Å), so the reduction in H_C is not due to a rapid growth of the particles. Instead, the temperature dependence of μ and H_C is related to the onset of the smooth transition of the majority fraction at T_{M2} towards a new magnetic state, as discussed below.

The small peak in $M(T)$ at $\simeq$120 K (Fig. 1) agrees with the behavior of H_C and μ. The fact that the rise in $M(T)$ on cooling does not level off, but instead it is followed by a decrease, supports the idea of a gradual strengthening of the AFM intracluster interaction. Therefore, the emergence of clusters is the source of both the deviation of the Curie-Weiss behavior at $T_{M1} \sim 230$ K (measured with $H = 1$ T) and the small peak in $M(T)$ detected $\sim$100 K below (measured with $H = 5$ Oe). The difference in temperature is due to the very smooth rise in $M(T)$ associated to the continuous increase of N and μ on cooling, and the different applied fields used in the measurements.

The variable density of clusters is related to the degree of oxygen depletion and the spatial distribution of the vacancies, determining the number of Ru^{4+} ions per cluster and the topological arrangement of the short Ru^{4+}–O–Ru^{4+} confined chains. On cooling, the emergence of a net magnetic moment and the onset of the canted AFM intracluster order gradually occur at different temperatures in the oxygen depleted regions. Therefore, the number of contributing particles to the magnetization in the virgin $M(H)$ branch rises for lower temperatures. This is the source of the smooth departure from the Curie-Weiss behavior observed below 230 K (see inset of Fig. 1), identified in the early works [11] as the higher magnetic transition temperature T_{M1}. The local character of the oxygen depleted regions, with no long-range chains of oxygen vacancies across the sample, stops the growth of the clusters beyond the immediate neighborhood around the oxygen vacancies. This assumption agrees with the good fit of

the $M(H)$ curves above T_{M2} with a single Langevin function, which indicates a narrow cluster size distribution. The lack of scaling observed for M/M_{sat} above T_{M2} is due to the complex nature of the cluster system, with a variable density of particles and a temperature dependent net magnetic moment. We note, however, that it does not explain why the hysteresis in the $M(H)$ loops, with an onset at T_{M1}, do not remain all the way down to low temperatures with an increasing (or at least constant) H_C. We will return to this point later.

The small volume fraction of the minority contribution and its nanometric size may cast some doubts whether it effectively comes from the Ru-1222 compound, or else due to a spurious phase undetected by the X-ray diffraction. However, the increase in the number of clusters with the decrease in temperature, as evidenced by our results, is difficult to be accounted by an impurity phase approach. Although it has been shown recently [21] that in the mixed Sr-Cu-Ru-O system a peak in $H_C(T)$ is obtained around 120 K, the magnitude of this peak strongly decreases with small variations in the Cu content around 10 at.% while the H_C values monotonically increase on cooling.

Let us now address the magnetic response below T_{M2}, for which a SG behavior was previously observed [12]. In this temperature region it is not possible to achieve good fits of the experimental $M(H)$ virgin branches with a single Langevin function, evidencing a distribution of SG-cluster sizes. In order to assess the average magnetic moment per cluster a superposition of Langevin functions with proper weights may be used [22,23]. The fitting of the virgin $M(H)$ branch at $T = 80$ K using three Langevin functions (not shown) gives for the contribution with a major weight a magnetic moment $\mu = 16 \times 10^3\ \mu_B$. This represents one order of magnitude larger than the cluster sizes deduced above T_{M2}. The other relevant feature is the excellent M/M_{sat} scaling with $(M_{sat}H)/T$ at 70 K $\leq T \leq$ 90 K (Fig. 4a). This result evidences the non-interacting character of the SG-clusters and is consistent with the vanishing of H_C in the same temperature interval (see Fig. 3). On cooling below 70 K, the change in the scaling factor of the M/M_{sat} curves, from $(M_{sat}H)/T$ to H/M_{sat}, evidences the transition to an interacting cluster-glass state, also supported by the reopening of the hysteresis in the $M(H)$ curves. In a previous report [12], the re-appearance of the hysteresis was interpreted as a signature of a spin re-arrangement going from a disordered state (SG phase) to a more ordered WFM state. We note that the H/M_{sat} scaling is excellent down to 10 K, showing that the cluster-glass state is preserved down to the lowest temperatures; the diamagnetic SC signal ($T_{SC} = 40$ K) is small in comparison to the dominant SG contribution. Since the evolution to an interacting SG state occurs ∼30 K above T_{SC}, a possible dipolar (AFM-like) coupling between the clusters, which would diminish the intensity of the internal magnetization at neighboring CuO_2 planes, would favor the onset of the SC state.

The dynamic response of the system is consistent with the dc measurements. Since the χ'-peaks occur near to $T = 80$ K (Fig. 5, inset), the failure of the Vogel-Fulcher type dependence to explain the frequency dependence of T_f is due to the non-interacting nature of the SG-cluster state for 70 K $\leq T \leq$ 90 K. The Vogel-Fulcher dependence was claimed to describe well the shift in T_f [12], suggesting the presence of magnetically interacting clusters at T_{M2}. However, a narrow frequency window of only three decades was used, for which an apparently satisfactory fitting can be achieved. Our measurements, with a frequency range of six decades, evidence a smooth but clear deviation from the Vogel-Fulcher dependence (see inset of Fig. 6). The Arrhenius-type dependence, which describes a system of non interacting particles with identical size, also fails because of the distribution of SG-cluster sizes, leading to a spread of relaxation times and to a superposition of frequencies responses [16,24]. Such size distribution is revealed by the need to employ several Langevin functions to fit the virgin $M(H)$ branches below T_{M2}.

In relation with the $H_C(T)$ dependence, we note that the Ru^{4+}-rich nano-islands scenario is consistent with its vanishing at T_{M2}. Since at the borders of the oxygen depleted regions there are Ru^{4+}-O-Ru^{5+} super-exchange interactions, the Ru^{4+}-clusters associated to the lack of stoichiometry become coupled to the rest of the Ru^{5+} moments as T_{M2} is approached, and absorbed into the larger non-interacting SG-clusters, with an anhysteretic magnetic response. The disappearance of a sizable coercivity of some tens of Oersted at T_{M2}, which in the case of a secondary impurity phase decoupled from the Ru^{5+} moments should be observable in a reversible SG background, strongly indicates that the Ru^{4+}clusters are actually incorporated into the Ru^{5+} SG ones. In a completely different approach, it has been suggested that the vanishing of H_C may be related to disorder at the RuO_2 layers induced by oxygen vacancies [12]. However, Al-doping in Ru-1222 compounds [9], also promoting disorder at the magnetic layers, do not induce any change in the $H_C(T)$ dependence in comparison to the parent compound.

Finally, in order to evidence the relevant role of the crystalline structure in the magnetic response it is worth comparing our results for Ru-1222 with a recent characterization of the Ru-1212 system [25]. Non-linear ac susceptibility measurements in Ru-1212 reveals the presence of a secondary magnetic structure just above the well known AFM-like transition. The results are compatible with the presence of FM nanoparticles. This assumption is confirmed by magnetization decay measurements, from which the mean volume of these particles was determined. In Ru-1222, the equilibrium between FM and AFM interactions is different, not only due to a larger separation between the RuO_2 layers, but also because the super-exchange chains are affected by the fact that the nearest-neighbor Ru ions are not vertically aligned [26]. As a consequence, magnetic frustration is enhanced, leading the observed cluster-glass state at a temperature T_{M2}, about 60 K lower than the AFM-like long-range transition in Ru-1212. Frustration also manifests itself in the size of the nanoclusters observed above the majority fraction transition, being approximately one order of magnitude smaller for Ru-1222. In both Ru-1212 and Ru-1222 systems the volume of the

minority fraction depends on annealing conditions. However, in Ru-1222 the oxygen stoichiometry can be varied in a wider interval, due to the presence of a R_2O_2 block [26], which promotes clustering at $T_{M1} \gg T_{M2}$. The large separation between these temperatures allowed our analysis of the $M(H)$ curves and the detailed characterization of the nanoclusters.

5 Conclusions

A scaling analysis of the magnetization yield a new insight about the nature of the magnetic state in Ru-1222, discarding on a quantitative basis the homogeneous multi-transitional model and the magnetic phase separation approach. The clear identification of the different magnetic species, all intrinsic to an optimum doped Ru-1222 sample, allowed us to reconcile previous contradictory results. The determined scaling factors and the change on cooling consistently account for the dynamic response and the temperature dependence of the coercive field. Magnetic frustration is a key point to understand the complex nature of nano-size clustering at high temperatures and the absence of long-range magnetic order at the lowest temperatures.

S.G. acknowledges financial support from CAPES, and CLAF (Latin American Center of Physics). S.S. was supported by CNPq. This research was funded by FAPERJ, CNPq, Israel Science Foundation (ISF, 2004 grant number: 618/04), and Klachky Foundation for Superconductivity.

References

1. J.W. Lynn, B. Keimer, C. Ulrich, C. Bernhard, J.L. Tallon, Phys. Rev. B **61**, 14 964 (2000)
2. Y. Tokunaga, H. Kotegawa, K. Ishida, Y. Kitaoka, H. Takagiwa, J. Akimitsu, Phys. Rev. Lett. **86**, 5767 (2001)
3. C.S. Knee, B.D. Rainford, M.T. Weller, J. Mater. Chem. **10**, 2445 (2000)
4. A.C. Mclaughlin, F. Sher, J.P. Attfield, Nature **436**, 829 (2005)
5. A.C. Mclaughlin, F. Sher, J.P. Attfield, Nature **437**, 1057 (2005)
6. I. Felner, U. Asaf, Y. Levi, O. Millo, Phys. Rev. B **55**, R3374 (1997)
7. I. Felner, U. Asaf, E. Galstyan, Phys. Rev. B **66**, 024503 (2002)
8. J. Dzyaloshisnky, J. Phys. Chem. Solids **4**, 241 (1958)
9. I. Felner, E. Galstyan, R.H. Herber, I. Nowik, Phys. Rev. B **70**, 094504 (2004)
10. A. Shengelaya, R. Khasanov, D.G. Eschenko, I. Felner, U. Asaf, I.M. Savić, H. Keller, K.A. Müller, Phys. Rev. B **69**, 024517 (2004)
11. Y.Y. Xue, B. Lorenz, D.H. Cao, C.W. Chu, Phys. Rev. B **67**, 184507 (2003)
12. C.A. Cardoso, A.J.C. Lanfredi, A.J. Chiquito, F.M. Araújo-Moreira, V.P.S. Awana, H. Kishan, R.L. de Almeida, O.F. de Lima, Phys. Rev. B **71**, 134509 (2005)
13. A. Butera, A. Fainstein, E. Winkler, J. Tallon, Phys. Rev. B **63**, 054442 (2001)
14. C.A. Cardoso, F.M. Araújo-Moreira, V.P.S. Awana, E. Takayama-Muromachi, O.F. de Lima, H. Yamauchi, M. Karppinen, Phys. Rev. B **67**, 020407(R) (2003)
15. P. Allia, M. Coisson, P. Tiberto, F. Vinai, M. Knobel, M.A. Novak, W.C. Nunes, Phys. Rev. B **64**, 144420 (2001)
16. E.F. Ferrari, F.C.S. da Silva, M. Knobel, Phys. Rev. B **56**, 6086 (1997)
17. N. Moutis, I. Panagiotopoulos, M. Pissas, D. Niarchos, Phys. Rev. B **59**, 1129 (1999)
18. J.M. De Teresa, M.R. Ibarra, P.A. Algarabel, C. Ritter, C. Marquina, J. Blasco, J. García, A. Del Moral, Z. Arnold, Nature (London) **386**, 256 (1997)
19. J.A. Mydosh, *Spin glasses: An Experimental Introduction* (Taylor & Francis, London, 1993)
20. M. Seeger, S.N. Kaul, H. Kronmüller, R. Reisser, Phys. Rev. B **51**, 12585 (1995)
21. I. Felner, E. Galstyan, I. Nowik, Phys. Rev. B **71**, 064510 (2005)
22. P. Allia, M. Coisson, M. Knobel, P. Tiberto, F. Vinai, Phys. Rev. B **60**, 12 207 (1999)
23. R.H. Yu, X.X. Zhang, J. Tejada, M. Knobel, P. Tiberto, P. Allia, J. Appl. Phys. **78**, 392 (1995)
24. M.A. Novak, W.S.D. Folly, J.P. Sinnecker, S. Soriano, J. Magn. Magn. Mater. **294**, 133 (2005)
25. M.R. Cimberle, R. Masini, F. Canepa, G. Costa, A. Vecchione, M. Polichetti, R. Ciancio, Phys. Rev. B **73**, 214424 (2006)
26. R.J. Cava, J.J. Krajewsky, H. Takagi, H.W. Zandbergen, R.B. Van Dover, W. F. Peck, Jr., B. Hessen, Physica C **191**, 237 (1992)